Zoological Journal of the Linnean Society, 2025, **205**(**4**), zlaf184
https://doi.org/10.1093/zoolinnean/zlaf184

OXFORD

Original Article

Intraspecific variation in osteoderm morphology in a cordylid lizard

Eleesha Annear[1,*], Lisa Van Linden[1], Jamie A. MacLaren[1,2,3], Simon Baeckens[1,4], Chris Broeckhoven[1], Raoul Van Damme[1]

[1]Functional Morphology Lab, Department of Biology, Universiteit Antwerpen, Antwerp, 2610, Belgium
[2]Evolution and Diversity Dynamics Lab, Department of Geology, Université de Liège, Liège, 4000, Belgium
[3]Palaeobiosphere Evolution Lab, Institute of Natural Sciences, Brussels, 1000, Belgium
[4]Earth and Life Institute, UCLouvain, Louvain-la-Neuve, 1348, Belgium

[*]Corresponding author. Functional Morphology Lab, Department of Biology, Universiteit Antwerpen, Antwerp, 2610, Belgium.
E-mail: eleesha.annear@uantwerpen.be, eleesha.annear@gmail.com

ABSTRACT

Osteoderms are bony elements in the dermis of a disparate set of vertebrates, including several taxa of reptiles. Why and to what extent osteoderms vary in occurrence, number, volume, and shape, particularly at the intraspecific level, remains poorly understood. Here we explored the extent of intraspecific variation in the cordylid lizard *Hemicordylus capensis*, which is broadly distributed across the Western Cape of South Africa. We sampled lizards from three geographically distinct populations along a longitudinal gradient and used micro-computed tomography and 3D geometric morphometrics to quantify osteoderm number, volume, and shape. Our results show substantial variation across populations, sexes, and body regions. Specifically, the northernmost population has significantly fewer and smaller osteoderms than the central and southern populations. We also observed sexual dimorphism: males have more and larger osteoderms than females. Interestingly, sexual shape dimorphism was restricted to the northern population, where males exhibit flatter, 'pancake'-shaped osteoderms and females more elongated, 'sausage'-like forms. Additionally, osteoderm morphology varied across body regions, with the neck bearing thicker, keel-shaped (often spiked) osteoderms, contrasting with the 'pancake'- or 'sausage'-shaped osteoderms on the trunk. We discuss potential functional interpretations for this variation—including roles in protection, thermoregulation, and hydroregulation—that merit further investigation.

Keywords: osteoderm, morphology, 3D geometric morphometrics, micro-computed tomography, Cordylidae, *Hemicordylus capensis*

INTRODUCTION

Osteoderms are the bony elements expressed in the skin of some groups of tetrapods (e.g. turtles, crocodiles, frogs, squamates, and mammals; Vickaryous and Sire 2009, Williams *et al.* 2022). They form part of the integumentary skeleton, and are composed mainly of calcium phosphate and collagen (Vickaryous and Sire 2009, Iacoviello *et al.* 2020). Osteoderms have been suggested to serve various functions (Ebel *et al.* 2025), including body protection (e.g. Broeckhoven *et al.* 2015, du Plessis *et al.* 2018), thermoregulation (e.g. Seidel 1979, Clarac and Quilhac 2019, Inacio Veenstra and Broeckhoven 2022), water retention (e.g. Broeckhoven *et al.* 2018a, b, c, Muñoz-Nolasco *et al.* 2019), and mineral storage (e.g. Dacke *et al.* 2015, Broeckhoven and du Plessis 2022). It is now well established that osteoderm expression (in terms of number or volume; Broeckhoven *et al.* 2015, Dacke *et al.* 2015) can vary widely among species (Williams *et al.* 2022), which may reflect adaptation(s) to specific ecological challenges, such as predation intensity (e.g. Broeckhoven *et al.* 2015), strong intraspecific (e.g. male-male) competition (e.g. Broeckhoven *et al.* 2017a, b, c, 2018a), and extreme climatic conditions (e.g. Broeckhoven *et al.* 2018b).

Recently, researchers have observed that the shape of osteoderms can also vary significantly (Maisano *et al.* 2019, Williams *et al.* 2022, Maliuk *et al.* 2024). Although these observations of shape variation in osteoderms have been mostly qualitative and based only on a limited number of species (Maisano *et al.* 2019, Williams *et al.* 2022, Maliuk *et al.* 2024), they suggest that morphological differences may reflect distinct functions driven by

Received 14 June 2025; revised 12 November 2025; accepted 20 November 2025

diverse selective pressures. For example, by comparison to other cordylid lizards, Armadillo girdled lizards (*Ouroborus cataphractus*) have evolved thicker osteoderms, possibly due to their greater exposure to predation when venturing farther from shelter (Janse Van Rensburg and Mouton 2009, Mouton 2011, Shuttleworth *et al.* 2013). Accordingly, their thick, sturdy osteoderms have been shown to withstand bites from predators such as mongooses (Broeckhoven *et al.* 2015). Beyond thickness, other aspects of osteoderm morphology may contribute to their strength and concomitant protective capacities. Keeled osteoderms better resist perpendicular forces or attacks (Sun and Chen 2013, Clarac *et al.* 2019), while discoid osteoderms are stiffer than elongated osteoderms, which are more elastic (Kéver *et al.* 2022) potentially influencing the trade-off between protection and mobility (Losos *et al.* 2002). Highly vascularized osteoderms may improve thermal capacity, facilitating thermoregulation and mineral storage, but could also reduce structural integrity, compromising their protective role (Broeckhoven *et al.* 2017b, Broeckhoven and du Plessis 2022). Ultimately, the presence, number, volume, size, shape, and distribution of osteoderms likely reflect trade-offs between these functions. However, fully understanding the functional and evolutionary drivers of osteoderm diversity requires a more detailed and quantitative analysis of their volume, number, shape, and variation within and across species.

While interspecific comparisons can certainly shed light on the evolution of traits, ecological and genetic divergences among species may confound ecomorphological studies. Comparisons among populations often allow more fine-tuned tests of how environmental differences drive phenotypic variation (Etterson *et al.* 2016). In addition, information on how traits vary at the organismal and populational level is pivotal to understanding and predicting a species' ability to cope with environmental change (Gamelon *et al.* 2025). In this respect, the graceful crag lizard (*Hemicordylus capensis*) offers a unique opportunity to study the evolution of osteoderms. In contrast to other species, in which the trait expression seems dichotomous (the species either expresses it or not), preliminary work has revealed interpopulational variation and sexual dimorphism in osteoderm expression in this widely distributed cordylid lizard (Cordylidae) (Broeckhoven *et al.* 2017a).

Recent advances in bio-imaging technology, such as micro-computed tomography (μCT), now allow for high-throughput, non-destructive 3D analyses of osteoderm anatomy in both museum specimens and live animals (Broeckhoven *et al.* 2017c, du Plessis *et al.* 2017, Maisano *et al.* 2019). These advancements facilitate a detailed exploration of intraspecific variation in osteoderm morphology.

In this study, we apply a high-resolution 3D imaging and morphology quantification approach to investigate variation in osteoderm volume, number, and shape in different body regions of males and females of *H. capensis* from populations across its distributional range. Our overarching aim is to understand how osteoderm morphology varies across populations, sexes, and across the body in *H. capensis*. In the absence of a detailed time series, this inter-populational variation provides a valuable proxy for studying trait evolution. We test three hypotheses: (i) environmental variation across the distribution range of *H. capensis* drives differences in osteoderm traits among populations. Here we predict that osteoderm number, volume, and shape varies across populations. (ii) Sexual selective pressures contribute to differences in osteoderm traits between males and females. We predict that males and females differ in osteoderm traits within populations. (iii) Osteoderm traits are functionally adapted to different selective pressures across the body (e.g. defence or mobility). Here we predict that osteoderm traits will vary across body regions.

MATERIALS AND METHODS

Study site and species

Hemicordylus capensis is a small cordylid lizard [snout-vent length (SVL): 93.33 ± 0.71 mm] endemic to South Africa, with a wide distribution ranging from Oorlogskloof Nature Reserve (31°29'S 19°03'E) in the north to Landdroskop (34°20'S 19°00'E) in the south and the Kamanassie mountains (33°37'S 22°54'E) in the south-east (Janse Van Rensburg 2009) (Fig. 1A).

The species is heliothermic and inhabits a diverse range of habitats, from cool montane regions to warm lowlands (Herselman *et al.* 1992, Janse Van Rensburg 2009). The species is strictly rupicolous, preferring medium to large boulders (Mouton and Van Wyk 1997, Janse Van Rensburg 2009), where individuals share rocks or boulders but partition space vertically based on demographic classes (Eifler *et al.* 2007). The territories of males rarely overlap with those of other males but often include female territories (Janse Van Rensburg and Mouton 2009).

To capture the full extent of intraspecific variation in osteoderm expression, we selected *H. capensis* populations across the distribution range of the species: (i) Oorlogskloof in the north (referred to as the northern population; 31°27'46"S, 19°04'43"E), (ii) Wolfberg in the Cederberg mountains (central population; 32°28'15"S, 19°16'32"E), and (iii) Swellendam in the Langeberg mountain range (southern population; 33°58'55"S, 20°28'23"E) (Fig. 1, Table 1).

The northern population is located at approximately 680 m a.s.l. on flat tableland, interspersed with deep gorges carved by rivers, where *H. capensis* inhabits sandstone escarpments. The region experiences summer temperatures of 14–29.7°C (seasonal minima and maxima temperatures) and winter temperatures of 4.9–17.9°C (Fick and Hijmans 2017). Rainfall ranges from 160–430 mm annually, occurring mostly in winter. The vegetation consists of bokkeveld sandstone fynbos (Northwest Fynbos Bioregion), characterized by restioid, proteoid, and asteraceous fynbos shrubs (Mucina and Rutherford 2011).

The central population inhabits a mountain peak at 1450 m a.s.l. in the rugged, dissected terrain of the Cederberg mountains, where *H. capensis* occurs on rocky outcrops and isolated peaks (Mucina and Rutherford 2011). The area is dominated by the Cederberg sandstone fynbos, with asteraceous and proteoid shrubs, while restioids are more common in deeper, moist sands (Mucina and Rutherford 2011). Rainfall is 180–600 mm annually, mostly between May and August. The climate is colder than the northern site, with summer temperatures of 11.1–24.9°C and winter temperatures of 1.8–13.1°C (Fick and Hijmans 2017).

The southern population is situated at 1179 m a.s.l. in the Langeberg mountains, characterized by a complex of gentle to steep south-facing slopes. The vegetation comprises ericaceous and restioid fynbos at higher elevations, transitioning into tall proteoid fynbos at mid to lower elevations, forming part of the

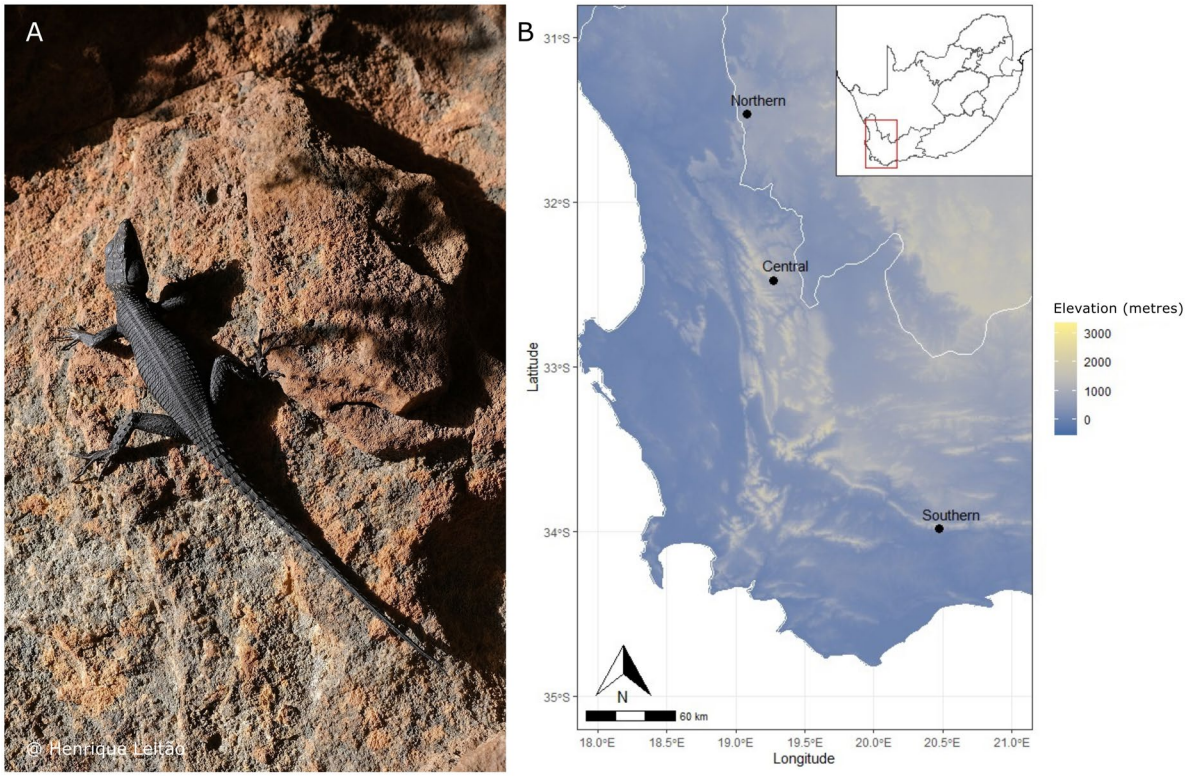

Figure 1. Image of an adult *Hemicordylus capensis* (sex unknown; photo courtesy of Henrique Leitão) representative of the central population (A) and a map of the study populations in South Africa showing the coordinates and elevations (metres) at which they occur (B).

Table 1. Snout-vent length (SVL) (mm), total osteoderm volume (OD vol) (mm^3), and number (OD nr) for males and females of the three *Hemicordylus capensis* populations studied

Population	N[a]	SVL[b] ± SE	OD vol[b] ± SE	OD nr[b] ± SE
Northern				
Males	20	101.75 ± 0.66	8.94 ± 1.93	153.65 ± 26.92
Females	11	101.43 ± 0.88	1.97 ± 0.61	53.09 ± 13.54
Central				
Males	20	88.21 ± 1.38	16.79 ± 3.29	309.60 ± 28.48
Females	11	90.32 ± 1.21	18.71 ± 5.31	337.82 ± 17.69
Southern				
Males	21	88.98 ± 0.92	12.44 ± 2.56	253.90 ± 18.01
Females	19	91.53 ± 0.85	12.12 ± 2.71	251.37 ± 23.31

[a]The sample size (N) is indicated.
[b]Values are averages ± SE.

South Langeberg Sandstone Fynbos (Mucina and Rutherford 2011). Rainfall varies widely from 320–1440 mm annually, with southeasterly winds bringing heavy clouds and mists at higher elevations (Mucina and Rutherford 2011). Temperatures range from 11.8–23.4°C in summer and 3.8–14°C in winter (Fick and Hijmans 2017).

Fieldwork

In October 2022, we caught a total of 102 adult *H. capensis* lizards (Table 1). Lizards were captured by noose or by hand and were transported in individual cloth bags in a cool box (± 20°C) to nearby temporary laboratory facilities. Upon arrival, we measured snout-vent length (SVL) using a digital calliper (CD-15CPX Mitutoyo, Germany; precision = 0.01 mm). DNA samples were collected from tail tissue of each individual, and sex was confirmed via genetic analysis (Leitão *et al.* 2023). Thereafter, lizards were transported in a portable incubator (± 20°C) to the Stellenbosch University µCT Scanner facility. (Permit numbers: CN44-87-18730; FAUNA-0843/2022; FAUNA-0844/2022).

Imaging osteoderms

At the Stellenbosch University scanning facility, we used micro-computed tomography (µCT) to acquire cross-sectional images of lizard osteoderms. µCT scanning was performed on live specimens following the protocols of du Plessis *et al.* (2017) and Broeckhoven *et al.* (2017c). To minimize movement, lizards were cooled for 30 minutes in an incubator set at 8°C prior to scanning; this temperature is above the critical thermal minimum for cordylid lizards (McConnachie *et al.* 2007). Cooled lizards were vertically restrained in a custom-built Styrofoam holder mounted on the rotating sample stage. We scanned whole-body specimens using a GE Phoenix v|tome|x L240 dual tube CT instrument (Phoenix X-ray, General Electric Sensing Technologies, Wunstorf, Germany) with the following parameters: 100 kV, 500 images, 250 ms capture time, 1 image averaged per rotation, 1 initial image skip. Each scan lasted 8.33 minutes, with a voxel size of 126 µm in the x- and y-axes.

Based on the scanning parameters used in our study, and following the radiation dose estimation approach of Broeckhoven *et al.* (2017a, b, c), the radiation dose received by the *H. capensis*

individuals was approximately 0.13 Gy. This value falls within the range typically reported for *in vivo* micro-CT imaging of small mammals and remains well below the LD_{50}(30) threshold for reptiles (Broeckhoven *et al.* 2017a, b, c). The *in vivo* micro-CT scanning protocol was approved by the ethics committee of both Stellenbosch University (numbers ACU-2021-2204; ACU-2022-2204) and the University of Antwerp (number ECD-dossier 2022-12). Each individual was scanned only once and subsequently released at their site of capture at the end of the micro-CT procedure.

Quantifying osteoderm expression and shape

To quantify osteoderm expression (as defined in Broeckhoven *et al.* 2015, Dacke *et al.* 2015), 3D renders of all osteoderms were extracted using ORS Dragonfly 2022.2. We extracted dorsal osteoderms (Fig. 2) embedded within the dermis and performed image segmentation using ORS Dragonfly 2022.2. Using reconstructed slice images, osteoderms were isolated along the trunk region from the base of the skull to the hip (i.e. up to the second sacral vertebra; Fig. 2). Based on the cordylid presacral vertebral formulae (Lang 1991; Supporting Information, Table S1), osteoderms were then categorized into four anatomical sections: (i) neck region (cervical vertebrae without ribs = 3), (ii) shoulder region (vertebrae with ribs but no sternal attachment = 5), (iii) trunk region (presacral vertebrae with sternal attachment and those posterior to the last sternal attachment = 18), and (iv) hip region (sacral vertebrae = 2). Total osteoderm volume (summed across all osteoderms within a selected anatomical region) was automatically calculated in the Basic Properties window of ORS Dragonfly 2022.2; osteoderm count (total number of distinct structures) was collated by summing the individual osteoderms within a given anatomical region.

To quantify osteoderm shape variation, we randomly extracted 3D osteoderm meshes (neck = 4, shoulder = 4, trunk = 8, hip = 4) from micro-CT scans and applied a geometric morphometric protocol using a high-density, semi-automated landmarking procedure (Fischer *et al.* 2022). Landmark- and semi-landmark-based geometric morphometric methods have been widely used to quantify skeletal morphology across both extant and extinct taxa (Lawing and Polly 2010, Mitteroecker and Schaefer 2022). Here, we adapted and applied semi-landmark-based techniques (e.g. Boyer *et al.* 2015, Fischer *et al.* 2022) to modern squamate osteoderms for the first time. Prior to landmarking, we isolated and decimated 3D scans of osteoderms to 50000 polygons in Geomagic Wrap 2017.0.1 to maintain consistency for automated

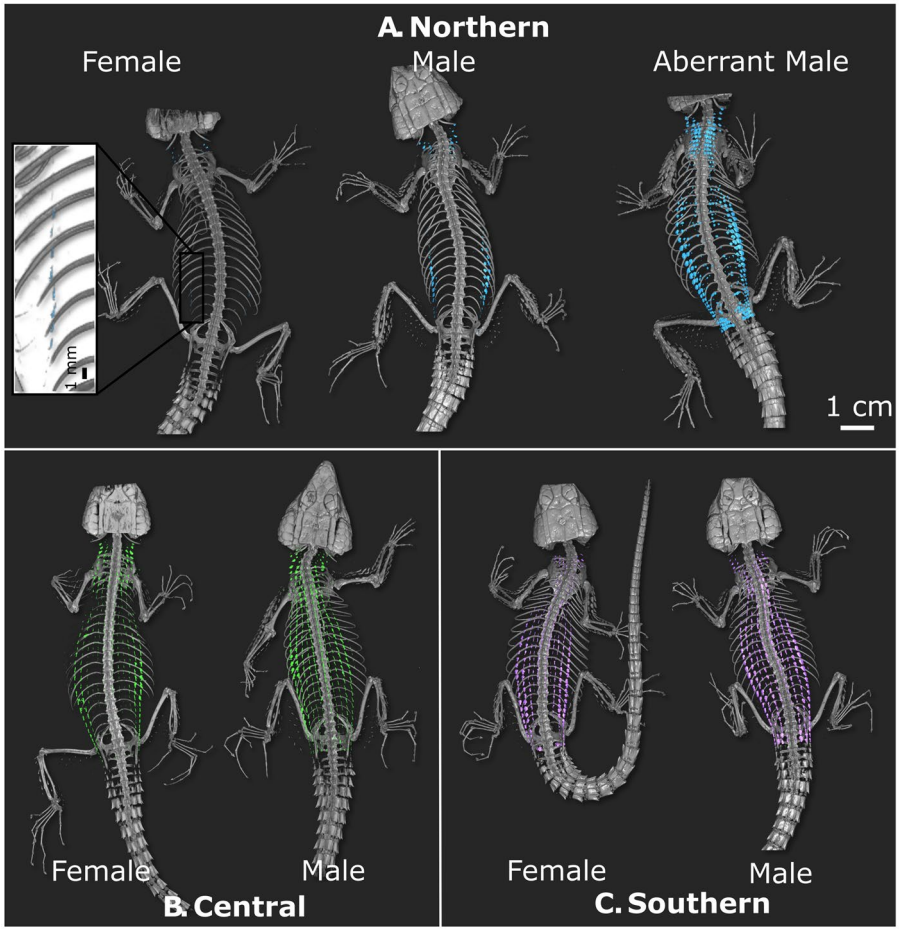

Figure 2. Micro-CT scans of males and females originating from the northern (A), central (B), and southern (D) populations of *Hemicordylus capensis*. Individuals shown exhibit osteoderm expression typical for their population and sex, except the northern male on the top right, which has an exceptionally large volume of osteoderms for that population (i.e. aberrant male). Osteoderms are presented in light blue, green, and purple to stand out visually for each of the different populations (northern, central, and southern, respectively).

landmarking, and re-meshed each surface in Geomagic Wrap to produce isotropic meshes (with polygons of comparable size), all-the-while retaining all morphological features.

The landmarking process involved four steps (see Supporting Information, Fig. S1). First, an atlas model was created by manually placing six fixed landmarks on a compressed sphere model, followed by the automated placement of 1500 surface semi-landmarks across the sphere's surface. This number was determined based on iteration trials to balance comprehensive surface coverage with computational efficiency. Second, the six fixed landmarks were manually placed on each osteoderm in Landmark Editor, after which the surface semi-landmarks from the atlas model were then iteratively patched onto the surface of each osteoderm, thus applying the semi-landmarks onto each unique osteoderm topology. Third, once all osteoderms were landmarked, the raw coordinates of all landmarks were ordinated using a Generalised Procrustes Analysis (GPA), removing the effect of orientation, location, and scale, and aligning all landmark configurations around a common geometric centre (centroid) (Zelditch *et al.* 2004). The resultant Procrustes distances were extracted and analysed using principal component analysis (PCA) to quantify major axes of shape variation. Fourth, due to the methodological artefact of over-sampling semi-landmarks along the sharp osteoderm edges in preliminary analyses, we selected the osteoderm with a shape plotting closest to the origin (0) for the initial PC1 vs. PC2 morphospace (accounting for 64.32%) and used that as a refined template model. We then repeated the landmarking procedure (steps 1, 2, and 3 above), using this average-shaped osteoderm as the template. The final dataset derived from this secondary landmarking procedure was used for statistical comparisons and visualizations. Semi-automated landmarking, GPA, and PCA were all performed in the R statistical software v.4.4.2 (R Core Team 2021).

Statistics

All analyses were performed with R statistical software v.4.4.2 (R Core Team 2021). We used a two-way analysis of variance (ANOVA) to test the effect of population and sex (and their interaction) on snout-vent length (SVL, log10-transformed). To test for sexual size dimorphism within each population, we used a Student's *t*-test.

We used generalized linear mixed models (*lme4* package; Bates *et al.* 2015) to test the effect of SVL, body region, population, and sex on osteoderm number, volume, and shape, with individual as a random factor. When overdispersion was detected in the model, we used an alternative mixed model that accounts for over- or under-dispersion in the data (*glmmTMB* package; Brooks *et al.* 2017). Due to the complex nature of the three-way interaction between body region, population, and sex, we conducted further analyses per body region with osteoderm number, volume, and shape as the response variables. We used negative binomial generalized linear models (nb-glm) for models with osteoderm number, and generalized linear mixed models (glmms) for models with osteoderm volume as the response variable, with SVL, population, and sex as predictor variables. We encountered issues with collinearity between SVL and its interactions with sex and population, which resulted in extreme variance inflation factors (VIFs). To combat this, we centred SVL to have a mean of 0 while maintaining variance (Kyriazos and Poga 2023). The same mixed models were also used for models with shape data as the response variable, and population and sex as the predictor variables, with individual as a random factor. The Akaike information criterion (AIC) was used for model selection in all cases (Burnham and Anderson 2004).

RESULTS

Sexual size dimorphism

Sexual size dimorphism varied significantly among populations (ANOVA on log10-transformed SVL, sex*population effect: $F_{2,403}$=4.267, P = 0.015). Females were on average significantly larger than the males in the central population (*t*-test, $t_{120.36}$ = 2.41, P = 0.02) and in the southern population ($t_{157.02}$ = 4.14, P < 0.001), but males and females did not differ in SVL in the northern population ($t_{90.08}$ = –0.61, P = 0.54).

Variation in osteoderm number and volume: whole body

Summing across all body regions, larger lizards had larger numbers of osteoderms in all three populations, but the size-effect was more pronounced in the northern population (nb-GLM, population*logSVL effect: χ^2_2 = 19.40, P < 0.001; Fig. 3A). Smaller northern lizards, in particular, had substantially fewer osteoderms than similar sized conspecifics of the southern and central populations. The size-effect was similar in males and females (sex*logSVL, χ^2_2 = 0.011, P = 0.91), but sexual dimorphism in osteoderm number differed significantly among populations (population*sex: χ^2_2 = 10.92, P = 0.004). Males had more osteoderms than females in the northern and southern populations, but the reverse was true in the central population (Fig. 3A).

Whole body total osteoderm volume increased with SVL in all three populations, but at a somewhat steeper gradient in the northern population (population*logSVL: χ^2_2 = 5.03, P = 0.08, Fig. 3B). Total volumes were low in the northern lizards by comparison to the central and southern lizards, especially for the smaller animals. Males tended to carry larger total volumes in the northern and southern populations, but not in the central population (population*sex: χ^2_2 = 4.85, P = 0.09, Fig. 3B).

The distribution of osteoderms over the four body regions (neck, shoulder, trunk, and hip) differed among populations (Fig. 3C–D). In the central and southern populations, more than 70% (by number and volume) were situated in the trunk region. In the northern population, and especially in the females of the northern population, this percentage was reduced in favour of the neck region (Fig. 3C–D). Below, we compare the number and total volume of osteoderms between sexes and populations, per body region.

Variation in osteoderm number and volume: body regions

Neck

In the neck region, osteoderm number increased with body size (nb-GLM, χ^2_1 = 42.59, P < 0.001) and this happened at a similar gradient in both sexes and all three populations (sex*log10SVL interaction effect: χ^2_1 = 1.96, P = 0.16; population*log10SVL: χ^2_2 = 1.97, P = 0.37). Males had more osteoderms than females in

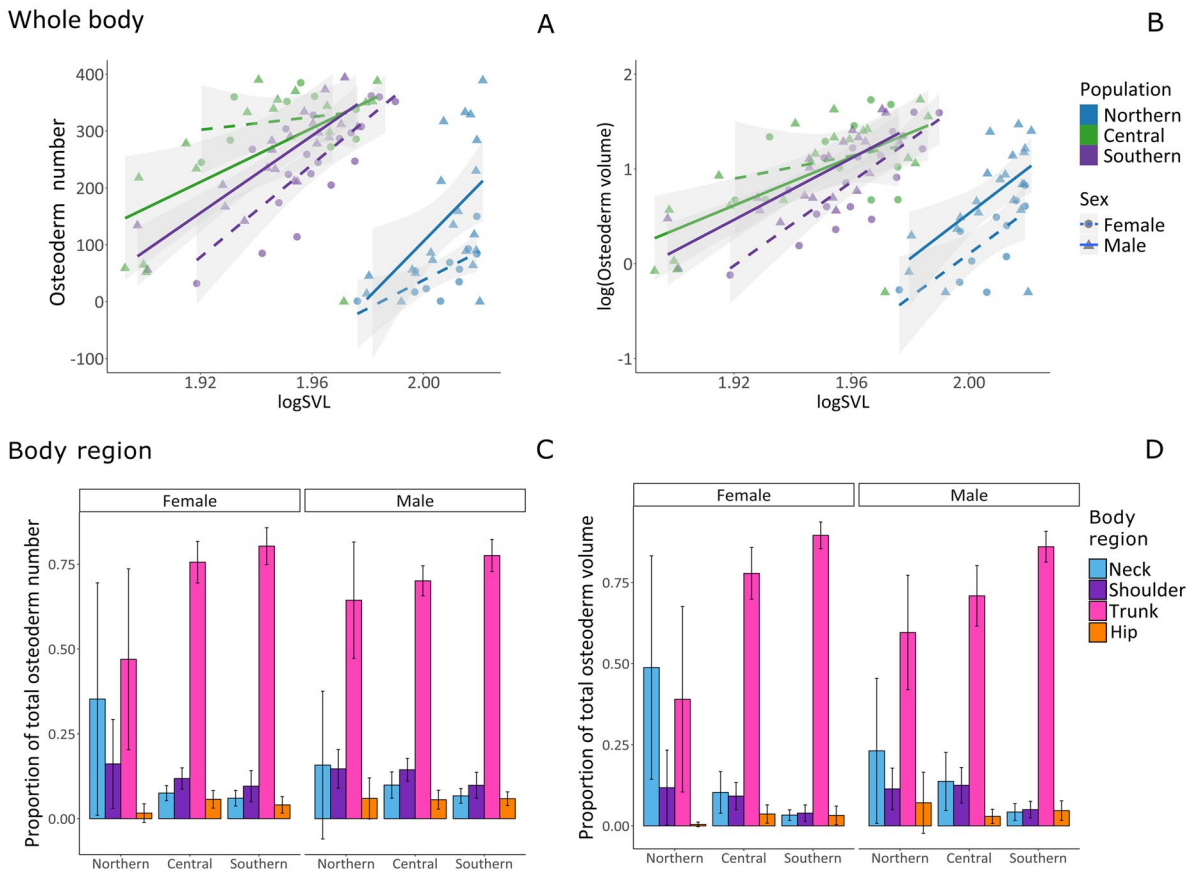

Figure 3. Number (A) and total volume (log-transformed) (B) of osteoderms (summed over all body regions) in male and female *Hemicordylus capensis* lizards from the three populations (northern: blue, central: green, southern: purple), as a function of snout-vent length (SVL, log-transformed). The distribution of the mean (± SD) proportion of osteoderm number (C) and volume (D) over the four body regions considered.

all three populations (effects of sex*population: χ^2_1 = 1.48, P = 0.47, sex: χ^2_2 = 9.68, P = 0.002). Populations exhibited considerable variation in the number of osteoderms (χ^2_2 = 134.70, P < 0.001), with the central population consistently having more neck osteoderms than the southern and northern populations, respectively (Fig. 4A).

Similar results were found for the total osteoderm volume in the neck region. Volume increased with body size (GLM, χ^2_1 = 69.63, P < 0.001) in a way that did not differ between sexes (χ^2_1 = 0.52, P = 0.77) or among populations (χ^2_2 = 4.49, P = 0.11). Males had larger volumes than females in all three populations (χ^2_1 = 13.43, P = 0.00025); the population*sex interaction was not significant (χ^2_2 = 3.62, P = 0.16). Individuals of the central population had larger volumes of osteoderms than the conspecifics from the southern and northern populations (χ^2_2 = 137.94, P < 0.0001, Fig. 4E).

Shoulder

The number of osteoderms in the shoulder region also increased with body size, with no significant differences between males and females (sex*log10SVL effect: χ^2_2 = 2.54, P = 0.28, Fig. 4B). However, there was a greater increase in osteoderm number in the northern (estimate = 52.9 ± 10.90, z = 4.85, P < 0.001) and southern populations (estimate = 14.15 ± 6.23, z = 2.27, P = 0.02) than in the central population (population*logSVL interaction effect, χ^2_2 = 22.7, P < 0.001; Fig. 4B). Males had more osteoderms than females in all three populations (population*sex interaction effect: χ^2_2 = 2.541, P = 0.28; effect of sex: χ^2_1 = 13.71, P = 0.00021, Fig. 4B).

The total volume of osteoderms in the shoulder region increased with body size (χ^2_1 = 69.83, P < 0.001), in a way that was similar in males and females (sex*logSVL effect: χ^2_1 = 2.12, P = 0.14; population*logSVL: χ^2_2 = 2.13, P = 0.34, Fig. 4F). Males in all three populations carried larger volumes of shoulder osteoderms (χ^2_1 = 13.71, P = 0.00021). Compared to the central population, lizards from the northern (estimate=-0.78 ± 0.085, z=-9.12, P < 0.001) and the southern population (estimate=-0.30 ± 0.054, z=-5.63, P < 0.001) had overall significantly smaller volumes of osteoderms in the shoulder region (χ^2_2 = 86.72, P < 0.0001, Fig. 4F).

Trunk

In the trunk region, osteoderm numbers increased with SVL with comparable patterns in males and females (sex*logSVL: χ^2_2 = 0.063, P = 0.80), although there was a notably steep gradient describing this relationship in the males of the northern

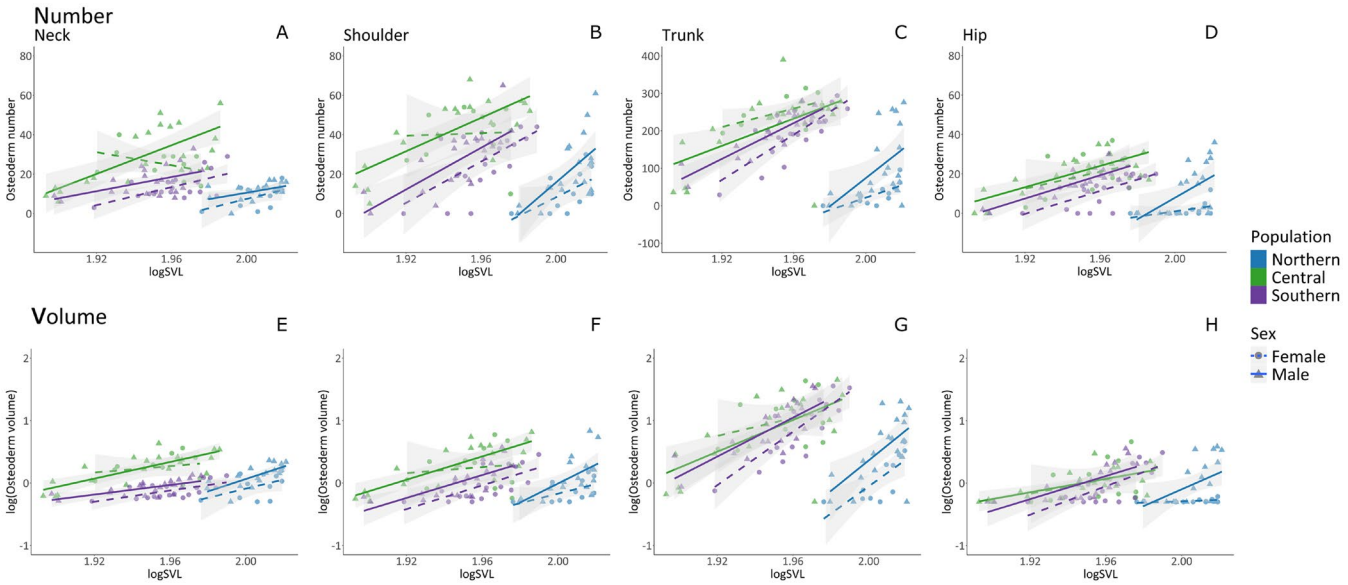

Figure 4. Number (A–D) and total volume (log-transformed) (E–H) of osteoderms in the neck (A, E), shoulder (B, F), trunk (C, G), and hip (D, H) regions of male (full line) and female (dashed line) *Hemicordylus capensis* lizards from the three populations (northern: blue, central: green, southern: purple), as a function of snout-vent length (SVL, log-transformed).

population (estimate (β) = 59.56 ± 10.48, z = 5.68, $P < 0.001$, Fig. 4C). Sexual dimorphism in the number of trunk osteoderms differed among populations ($\chi^2_2 = 17.37$, $P = 0.00017$); while in the northern and southern populations males carried more osteoderms than females, the reverse was true for the central population. Overall, individuals from the northern population had fewer osteoderms than those from the southern and central populations (population main effect: $\chi^2_2 = 86.59$, $P < 0.0001$, Fig. 4C).

Variation in total osteoderm volume at the level of the trunk followed similar patterns to the osteoderm numbers. Larger lizards had larger osteoderm volumes, with no significant effect of sex (sex*logSVL interaction effect: $\chi^2_2 = 0.001$, $P = 0.99$, Fig. 4G). Osteoderm volume increased with SVL in the northern population with a steeper gradient (estimate = 11.84 ± 5.65, z = 2.10, $P = 0.039$) than in the central population. The southern and central populations did not differ in this respect (estimate = 6.07 ± 3.80, t = 1.60, $P = 0.11$). The sexual dimorphism in osteoderm volume varied significantly among populations (population*sex: $\chi^2_2 = 7.15$, $P = 0.028$); as with osteoderm number, females recorded larger osteoderm volumes than males in the central population, but not in the northern and southern populations. Overall, northern lizards had smaller trunk osteoderm volumes than southern and central lizards (population main effect: $\chi^2_2 = 67.52$, $P < 0.0001$, Fig. 4G).

Hip

As in the trunk region, the number of osteoderms in the hip region increased with SVL in all populations, but more steeply in the northern population (estimate = 100.58 ± 20.94, z = 4.80, $P < 0.001$; population*logSVL interaction effect: $\chi^2_2 = 22.80$, $P < 0.0001$, Fig. 4D). The effect of SVL on the hip osteoderm number was not significantly different between males and females ($\chi^2_1 = 0.003$, $P = 0.96$). Sexual dimorphism in hip osteoderms varied among populations ($\chi^2_2 = 15.22$, $P = 0.0005$); males had more osteoderms than females in all three populations, but the difference between sexes was much larger in the northern population (Fig. 4D).

As for the volume of hip osteoderms, the effect of SVL showed no significant differences for males and females (sex*logSVL interaction effect: $\chi^2_1 = 0.046$, $P = 0.83$) in all three populations (population*logSVL interaction effect: $\chi^2_2 = 3.82$, $P = 0.15$, Fig. 4H), despite the northern population females having very few osteoderms. Males had larger volumes than females in all three populations (population*sex interaction effect: $\chi^2_2 = 3.93$, $P = 0.14$, sex-effect: $\chi^2_1 = 9.76$, $P = 0.0018$). Individuals from the northern population (especially females) had much fewer hip osteoderms than those from the southern and central populations (population main effect: $\chi^2_2 = 44.82$, $P < 0.0001$, Fig. 4H).

Variation in osteoderm shape

Principal component analysis of the Procrustes distances produced two composite variables that jointly captured 64.65% of the total variation (Fig. 5). Osteoderms with negative scores on PC1 (56.48%) were flat and discoid ('pancake'-shaped), while those with positive scores were anteroposteriorly elongated ['sausage'-shaped, comparable to the 'vermiform' osteoderms described in *Varanus komodoensis* (Maisano *et al.* 2019)]. The second axis (8.17%) separated osteoderms with pronounced dorsal keels ('spike'-like, with positive scores) from flat osteoderms with smooth dorsal regions (negative scores; Fig. 5; example osteoderms in Fig. 5B–D). PC1-scores varied in a complex way among body regions, populations, and sexes (GLM, three-way interaction: $\chi^2_6 = 66.64$, $P < 0.0001$); as a result, we ran analyses per body region, as we did for osteoderm number and volume. Our analysis of PC2-scores did not reveal such a three-way interaction effect ($\chi^2_6 = 7.64$, $P = 0.27$), but the body region*population effect was highly significant ($\chi^2_6 = 48.21$, $P < 0.0001$). For clarity, we will also report results per body region for PC2.

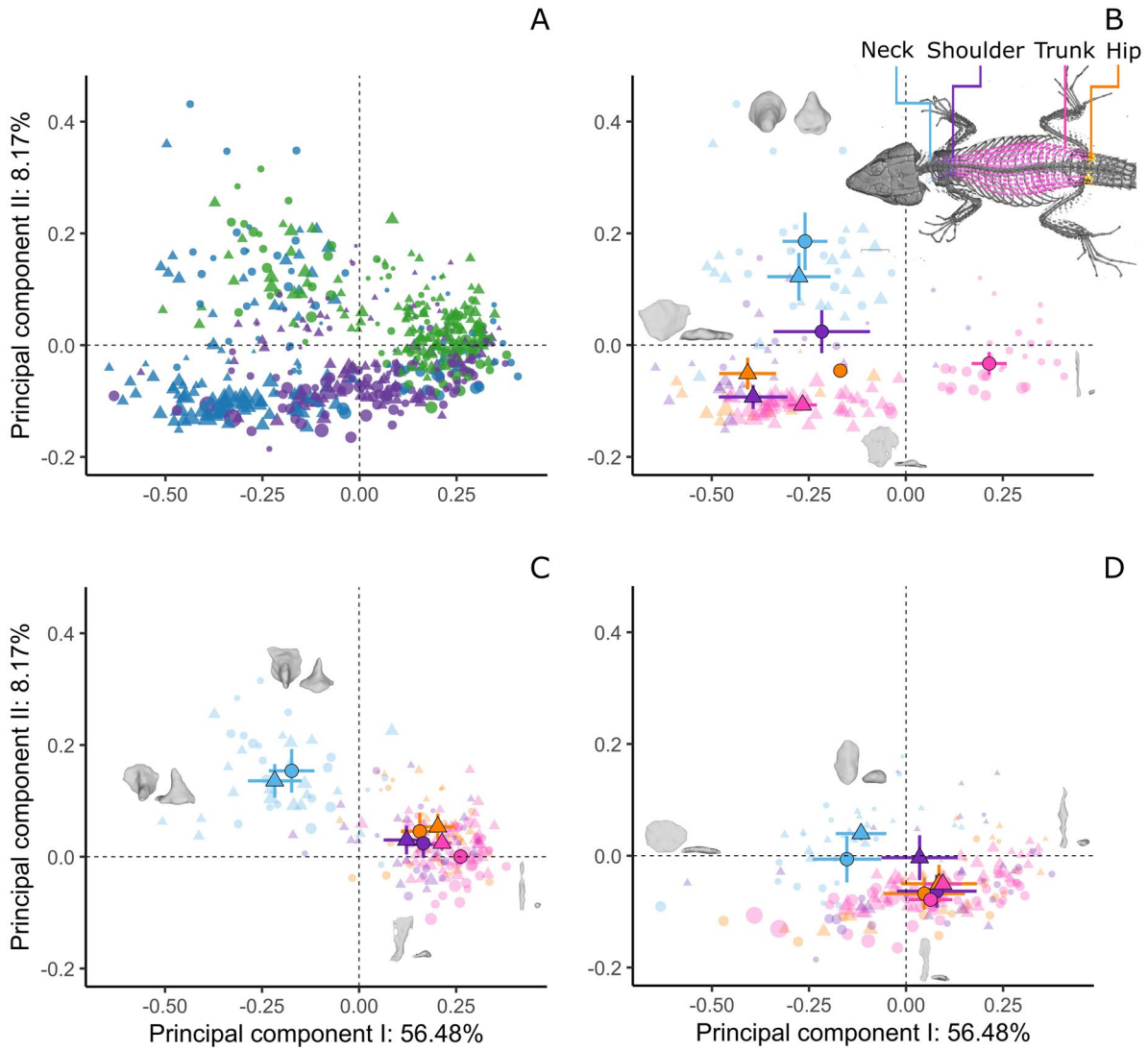

Figure 5. Principal components analysis (PCA) of osteoderm shape across three populations of *Hemicordylus capensis*. PCA plot showing the first two principal axes, representing 56.48% (PC1) and 8.17% of the variation (PC2) for all populations (northern: blue, central: green, southern: purple) and sexes (male: triangle, female: round) (A). Population-specific PCA plots (based on same axes) for the northern (B), central (C), and southern (D) populations, with representative osteoderms illustrating osteoderm shape variation along each axis. All points originate from the same PCA (A) but are separated by population in (B–D). Mean PC-values for each body region are indicated by the larger, bold-coloured data points, with 95% confidence intervals for each axis. The light-shaded points represent individual osteoderm values scaled to osteoderm centroid size and females are represented by circles, males by triangles. Colours in (B–D) indicate body regions; neck (blue), shoulder (purple), trunk (pink), and hip (orange).

Neck

Neck region osteoderms scored low on PC1, indicating that they tend to be more pancake-shaped (Figs 5, 6A). Sex did not affect PC1-scores for neck osteoderms, neither in interaction with population (population*sex effect, $\chi^2_2 = 1.18$, $P = 0.55$), nor in isolation ($\chi^2_1 = 0.07$, $P = 0.79$). PC1-scores did differ between populations ($\chi^2_2 = 12.87$, $P = 0.0016$; Fig. 5); they were most negative in the northern population, intermediate in the central population, and least negative in the southern population (Fig. 6A). Variation along PC2 was due to population differences only ($\chi^2_2 = 35.86$, $P < 0.0001$; Fig. 5B–D). Scores for the southern population were much lower (lower keels) than those of the central and northern populations (stronger keels). Sex had no effect on 'keeledness' of the osteoderms (population*sex: $\chi^2_2 = 5.07$, $P = 0.07$; sex: $\chi^2_1 = 0.35$, $P = 0.55$, Fig. 6E).

Shoulder

Shoulder region osteoderms were more elongate and sausage-shaped in the central and southern population, but round and pancake-shaped in the northern population (population-effect on PC1 scores: $\chi^2_2 = 66.38$, $P < 0.001$, Figs 5B–D, 6B). The variation in PC1-scores for shoulder osteoderms was not affected by sex, either in isolation ($\chi^2_1 = 3.01$, $P = 0.08$) or in interaction with population ($\chi^2_2 = 1.85$, $P = 0.40$).

PC2 scores for the shoulder osteoderms exhibited remarkable population-specific sexual dimorphism (population*sex

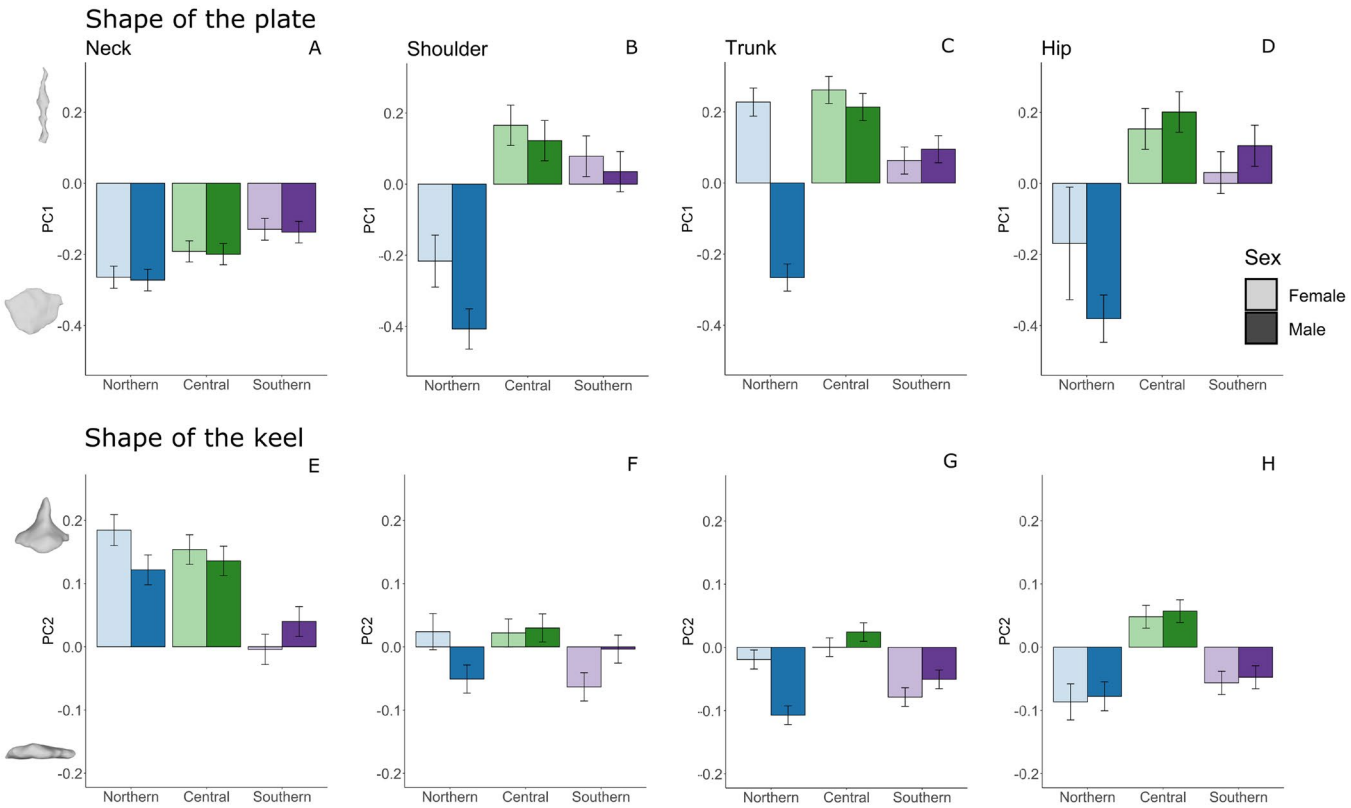

Figure 6. Osteoderm shape variation in male and female *Hemicordylus capensis* lizards from the three populations. Shown are average (± SE) projections on the first (A–D) and second (E–H) principal component (PC) axes for the neck (A, E), shoulder (B, F), trunk (C, G), and hip (D, H) regions. Positive scores on PC1 reflect sausage-shaped osteoderms, negative scores on PC1 reflect pancake-shaped osteoderms, and positive scores on PC2 reflect more strongly keeled osteoderms. Exemplar osteoderms shown on left in dorsal aspect (A–D) and lateral aspect (E–H).

interaction effect, $\chi^2_2 = 7.89$, $P = 0.02$), particularly in two populations. In the northern population, females scored higher than males, but the reverse was true in the southern population (Fig. 6F). Males and females of the central populations both had positive scores (indicative of strong keels).

Trunk

Trunk osteoderms exhibited population-dependent sexual dimorphism in shape (population*sex interaction effect on PC1, $\chi^2_2 = 53.85$, $P < 0.0001$; Fig. 6C). The northern population stood out: trunk osteoderms of males scored low on PC1, indicating a pancake shape (Fig. 5B). In contrast, trunk osteoderms of female northern lizards, and those of both males and females of the central and southern populations, had positive PC1 scores representative of sausage shapes (Figs 5B–D, 6C).

Scores for the trunk osteoderms on PC2 also exhibited a population*sex interaction effect ($\chi^2_2 = 19.82$, $P < 0.05$). Scores were mostly near-0 or negative (flat, unkeeled), but more so in northern males and southern lizards of both sexes (Fig. 6G).

Hip

Hip osteoderms differed in shape among populations ($\chi^2_2 = 51.46$, $P < 0.0001$, Fig. 6D); their PC1-scores were mostly positive (indicative of sausage-like shapes) in the central and southern population, but negative in the northern population (suggesting pancake-like shapes; Fig. 5). Variation in hip osteoderm PC1 scores was not significantly affected by sex ($\chi^2_1 = 0.38$, $P = 0.54$) or any population*sex interaction ($\chi^2_2 = 2.33$, $P = 0.31$).

PC2 scores of hip osteoderms varied among populations only ($\chi^2_2 = 34.60$, $P < 0.0001$, Fig. 6H), indicating more prominent keels in the central population, but not in the two other populations (Fig. 5). Sex did not explain variation in these scores, neither in isolation ($\chi^2_1 = 0.19$, $P = 0.66$) nor in interaction with population ($\chi^2_2 = 0.69$, $P = 0.71$).

DISCUSSION

Our analyses on *Hemicordylus capensis* reveal substantial variation in osteoderm volume, number, and shape among populations, between sexes, and across body regions, supported by our hypotheses. Although we found a few consistent patterns across all populations, for example, neck osteoderms tended to be pancake shaped regardless of sex or population, our results overall reveal substantial variability within and among individuals and populations. While such variation may result from both adaptive and non-adaptive processes, our current dataset does not permit definitive conclusions about its evolutionary origins or the mechanisms driving it. Nonetheless, certain patterns in osteoderm expression and morphology hint at possible functional roles and adaptive significance, which motivates us to explore potential adaptive explanations for the observed differences.

Protection against conspecifics

We found that males generally possessed higher osteoderm numbers and volumes than females, supporting our second hypothesis. One possible explanation for some of the observed patterns in osteoderm variation is the presumed differing exposure to intraspecific aggression, and thus variation in the need for bodily protection, known as the 'fighting-advantage' hypothesis (Broeckhoven 2022, Frýdlová *et al.* 2025). While interpretations remain speculative without thorough functional or biomechanical data, here we elaborate upon our morphological results within this framework.

Sex-based differences in osteoderm morphology may reflect divergent selective pressures acting on males and females. Sexual dimorphism is widespread in lizards, with males typically exhibiting larger body sizes, more robust heads, and greater bite forces, characteristics often associated with intra-sexual competition and mate acquisition (Olsson *et al.* 2002, Cox *et al.* 2003). However, Van Wyk and Mouton (1998) showed that *H. capensis* does not follow this general trend of sexual dimorphism in lizards. In *H. capensis*, females have larger body sizes than males (Supporting Information, Fig. S2), while males have relatively larger heads. These patterns raise two questions: first, are females prioritizing traits linked to reproductive output (i.e. fecundity selection; Olsson *et al.* 2002), potentially at the expense of dermal armour? Second, is there a relationship between the male-plus dimorphism in head size (which is commonly used as a proxy for bite force, see Herrel *et al.* 2001) and the male-plus dimorphism in osteoderm traits? Indeed, *H. capensis* is a territorial species, and male territories rarely overlap. While females are less territorial, aggressive encounters involving female-female, female-juvenile, and female-male interactions have been documented (Eifler *et al.* 2007, Janse Van Rensburg and Mouton 2009). Thus, although we found that males generally had higher osteoderm numbers and volumes, the presence of observed aggressive interactions in both sexes suggests that osteoderms as protection may benefit all individuals, albeit to differing degrees depending on life-history priorities.

Furthermore, the higher relative osteoderm investment in the neck, and trunk regions, supports our third hypothesis. We found that the proportions of osteoderm numbers and volumes are high in body regions typically targeted by conspecific attacks (i.e. neck and trunk), potentially suggesting a need for increased protection in these areas across all three populations. In addition, the largest osteoderms are also typically located in the lateral rows of the trunk (Fig. 7). Combat in cordylid lizards typically involves lateral positioning, with two lizards circling each other in a face-off that includes various display tactics before attempting to bite the opponent's trunk or neck (Broeckhoven *et al.* 2017a). Among the four anatomical body regions examined in this study, the neck and trunk appear to be the most vulnerable with both regions containing vital organs and major blood vessels integral for survival. The osteoderms in the neck and trunk may help distribute localized forces from bites, whether inflicted by a predator or conspecific, across a broader area (Yang *et al.* 2013), potentially preventing damage to underlying soft tissue and vital organs. In the case of the neck, we observed that the osteoderms occurring

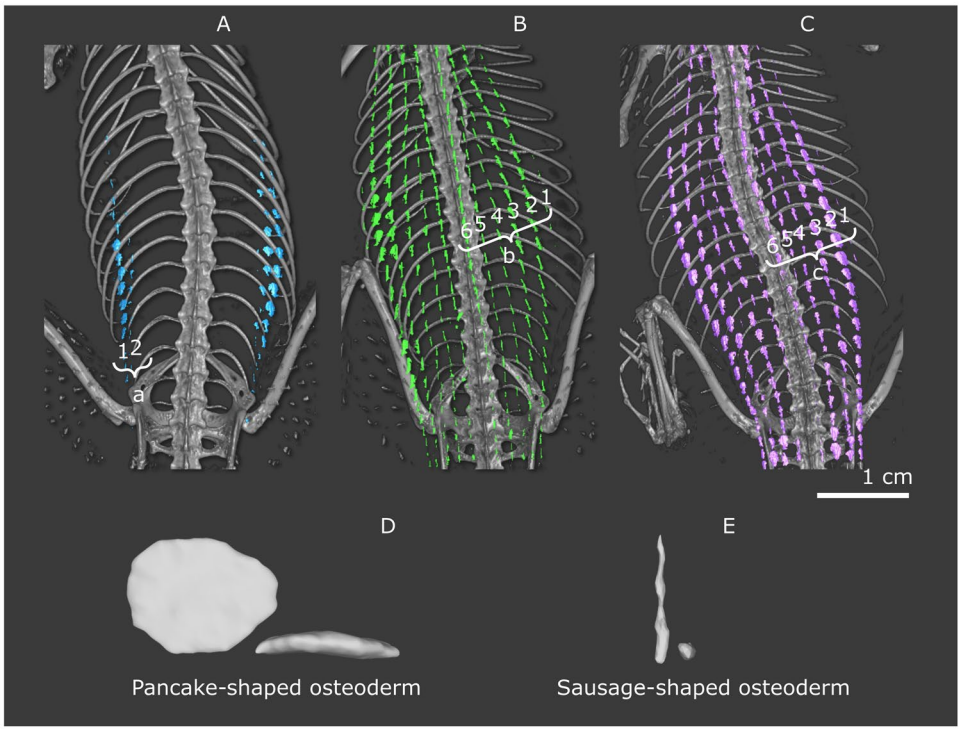

Figure 7. Osteoderm morphology and distribution pattern in the trunk of male *Hemicordylus capensis* lizards from the northern (A), central (B), and southern (C) populations. The number of rows exhibited by typical males of the populations is indicated (a, b, and c). Additionally, examples of pancake-shaped (D) and sausage-shaped (E) osteoderms are provided and can be seen in the 3D-rendered images of the three males. Osteoderms are presented in blue, green, and purple to stand out and visually denote the population of origin (from left: northern, central, and southern).

in this area are strongly keeled and predominantly discoid in shape. Keeled osteoderms are better at resisting perpendicular forces from bites or attacks (Sun and Chen 2013, Clarac *et al.* 2019), whereas discoid osteoderms are stiff (Kéver *et al.* 2022), and allow for a larger surface area to be covered by the bony plate of the osteoderm. Combined, these characteristics enhance the protective function of the osteoderm within the neck region. Moreover, the variation in osteoderm morphology observed in *H. capensis* may reflect different protective strategies: a dense, high-volume arrangement may reduce the likelihood of skin penetration, whereas a targeted investment in specific key locations could help absorb impact and minimize internal injury during attacks (Fig. 7).

Protection against predation

The late onset of trunk osteoderm development (Vickaryous and Hall 2008, Broeckhoven *et al.* 2015, 2017a) suggests that these osteoderms are less likely to serve as primary protection against predators (Ebel *et al.* 2025). However, we do not dismiss the possibility that osteoderms provide secondary defence against predation. An extensive distribution of osteoderms could enhance protection by making it harder for some predators to easily bite or handle their prey (Shine 1998, Greer 2007, Broeckhoven *et al.* 2015). The osteoderm traits observed in *H. capensis* are unlikely to withstand the bites of birds of prey or mongooses (Broeckhoven *et al.* 2015). However, if osteoderms do serve an antipredator function in this species, it may be primarily against snake predation (Broeckhoven *et al.* 2015). Although direct evidence of snake predation on *H. capensis* is scarce, it is known that various snake species predate on cordylid lizards (e.g. Shine *et al.* 2006, 2007, Parusnath 2012, Taft *et al.* 2017). The snakes are generally able to reach the lizards inside the rock crevices; however, increased osteoderm expression and larger keeled shapes would make it more difficult for the snakes to extract the lizards from the crevice. Additionally, populations inhabiting vertical rock facades, such as those in the north, may experience reduced exposure to snakes and thus require less dermal armour than southern populations that occupy flatter, more accessible rocky habitats closer to the ground. Consequently, the lower osteoderm expression in the northern population may reflect reduced snake predation pressure. This could be due to lower predator richness, or abundance, differences in predator composition, or greater availability of shelter in the habitat. This north-south contrast in osteoderm morphology provides partial support for the first hypothesis, although direct data on predator abundance, and attack rates are needed to confirm causality. In addition to data on predator occurrence and habitat structure, testing this hypothesis will also require observations on the lizards' escape tactics, as osteoderms may protect against predation, but may also reduce running velocity (Losos *et al.* 2002).

Thermo-/hydroregulatory function

In addition to their (seemingly intuitive) role in organismal protection, osteoderms may also contribute to thermoregulation, with variation in their volume, number, and shape potentially reflecting subtle adaptations in local thermal environments. In the past, two main hypotheses have been proposed: the first posits that osteoderms facilitate heat exchange due to their vascularization, which could allow for controlled heat dissipation or absorption (Clarac *et al.* 2017, Clarac and Quilhac 2019). However, vascularization has also been associated with other physiological roles, such as calcium storage and mobilization (Dacke *et al.* 2015, Broeckhoven and du Plessis 2022), making this interpretation context-dependent. The second hypothesis proposes that osteoderms act as thermal insulators, buffering the animal from extreme temperatures due to the inherently low thermal conductivity of bone (Inacio Veenstra and Broeckhoven 2022). For osteoderms in *H. capensis* to serve a heat-exchange function, vascularization would be a prerequisite (Seidel 1979, Ebel *et al.* 2025). However, nano-CTs of osteoderms of this species have revealed no evidence of vascular structures (C. Broeckhoven, personal communication). However, to confidently rule out the heat-exchange and calcium-facilitatory functions, histological data would need to confirm this observation.

Alternatively, these osteoderms may function as thermal insulators, impeding heat exchange by acting as a physical barrier. The limited osteoderm expression observed in this study in the northern population (restricted to a single, occasionally duplicated, dorsolateral line) implies a negligible role for these osteoderms in thermoregulation. Their restricted distribution would likely have minimal impact on heat retention. Notably, individuals in this population are also significantly larger in body size and occupy warmer environments. This pattern may represent a compensatory shift, where increased body mass (consistent with Bergmann's rule) and relatively higher ambient temperatures may provide a similar insulating effect to that offered by more extensive osteoderm coverage (Zamora-Camacho *et al.* 2014). In contrast, the central and southern populations possess sausage-shaped osteoderms that are more broadly distributed across the dorsal trunk. In colder environments, such a configuration may offer enhanced insulation, potentially reducing heat loss and allowing individuals to extend their active periods for foraging and other activities. Additionally, the greater diversity of osteoderm shapes in the southern population could reflect adaptation to a wider range of environmental effects, whereas the more uniform osteoderm shapes in the central population may indicate a response to a relatively stable thermal regime. Taken together, these climate associated differences in osteoderm volume, number, and shape provide partial support for the first hypothesis, even if the precise mechanism remains to be verified.

Aside from protection and thermoregulation, osteoderms have been hypothesized to play a role in water retention, particularly in arid environments (Broeckhoven *et al.* 2018a, c). Although their direct effect on evaporative water loss has not yet been tested, previous studies have reported strong correlations between osteoderm volume and environmental aridity in cordylid lizards (Broeckhoven *et al.* 2018a, c, Muñoz-Nolasco *et al.* 2019). Interestingly, among the three populations examined in this study, only the northern population (characterized by highly reduced osteoderm expression) regularly occurs near water bodies, such as rivers (Janse Van Rensburg 2009, Janse Van Rensburg and Mouton 2009). In contrast, the central and southern populations, which show greater osteoderm investment in terms of volume, number,

and shape, inhabit isolated mountain peaks with limited access to surface water. This spatial pattern raises the possibility that *H. capensis* osteoderms may contribute to hydroregulation, particularly in populations exposed to more xeric conditions, and provides further partial support for the first hypothesis. However, if osteoderms function solely in hydro- or thermoregulation, it remains unclear why these traits would exhibit sexual dimorphism.

Given the number of (not mutually exclusive) roles that osteoderms may play, it cannot be concretely stated that the *H. capensis* populations examined in this study have osteoderms adapted for any one specific function. The high degree of variability in the osteoderm number, volume, and shape across populations and within individuals of this cordylid hints at there being a mosaic of influences on osteoderm expression. Each osteoderm may therefore fulfil primary, secondary, and even tertiary roles depending on ecological and physiological context. It is thus important to consider how these potential functions may interact to influence osteoderm expression. For example, in warmer climates such as those inhabited by the northern population, lizards shuttle up and down a vertical surface for efficient thermoregulation (Huey and Pianka 1977). This behavioural thermoregulatory strategy may be particularly important for melanistic lizards (Clusella-Trullas *et al.* 2009). However, rapid vertical movement may increase exposure to aerial predators against which osteoderms offer little to no protection. This increased predation risk during movement may impose strong selective pressure against extensive osteoderm expression (Losos *et al.* 2002).

Conclusion

In this study, we have demonstrated that a quantitative, pseudo-landmarking procedure can be successfully modified to analyse complex structures like osteoderms, in order to draw inferences on functional morphology and population-level variation. We propose that the shape data generated by this method may provide more accurate assessment of osteoderm (functional) morphology than simple categorization or volume measurements alone. Using this framework, we show substantial intraspecific variation in osteoderm morphology in *H. capensis*, including differences in osteoderm number, volume, and shape across sexes, body regions, and populations. While we cannot draw firm conclusions about the selective drivers of this variation, we outline several potential functional interpretations, such as protection, thermoregulation, and hydroregulation, that warrant further investigation.

The 3D data presented here provide a robust quantitative foundation for future research into the mechanical and physiological roles of osteoderms within a phylogenetic context. Further behavioural, functional, and comparative studies integrated with ecological and genomic data, will be essential to clarify the selective pressures shaping osteoderm evolution in *Hemicordylus* and other squamate lineages.

ACKNOWLEDGEMENTS

We acknowledge the support of Jan Scholliers, Jorrit Mertens, Henrique Leitão, Dave Van Landeghem, Alexandros Bantounas, and Genevieve Diedericks during data collection, and that of Cang Hui for facilitating the application for an ethical permit with Stellenbosch University. The authors thank Christophe Mallet, Torsten Scheyer, and Edward Stanley for insightful conversations. This research was supported by funding from the University of Antwerp.

SUPPLEMENTARY DATA

Supplementary data is available at *Zoological Journal of the Linnean Society* online.

CONFLICT OF INTEREST

The authors have no conflict of interest.

FUNDING

Funded by the University of Antwerp Bijzonder Onderzoeksfonds-Geconcerteerde Onderzoeksacties (BOF-GOA):0004233.

DATA AVAILABILITY

The data underlying this article are available in Figshare at http://dx.doi.org/10.6084/m9.figshare.29314739.

REFERENCES

Bates D, Mächler M, Bolker B *et al.* Fitting linear mixed-effects models using lme4. *Journal of Statistical Software* 2015;**67**:1–48.

Boyer DM, Puente J, Gladman JT *et al.* A new fully automated approach for aligning and comparing shapes. *Anatomical Record* 2015;**298**:249–76.

Broeckhoven C. Intraspecific competition: a missing link in dermal armour evolution? *The Journal of Animal Ecology* 2022;**91**:1562–6.

Broeckhoven C, du Plessis A. Osteoderms as calcium reservoirs: insights from the lizard *Ouroborus cataphractus*. *Journal of Anatomy* 2022;**241**:635–40.

Broeckhoven C, de Kock C, Hui C. Sexual dimorphism in the dermal armour of cordyline lizards (Squamata: Cordylinae). *Biological Journal of the Linnean Society* 2018b;**125**:30–6.

Broeckhoven C, de Kock C, Mouton PlFN. Sexual dimorphism in osteoderm expression and the role of male intrasexual aggression. *Biological Journal of the Linnean Society* 2017a;**122**:329–39.

Broeckhoven C, Diedericks G, Mouton PlFN. What doesn't kill you might make you stronger: functional basis for variation in body armour. *The Journal of Animal Ecology* 2015;**84**:1213–21.

Broeckhoven C, El Adak Y, Hui C *et al.* On dangerous ground: the evolution of body armour in cordyline lizards. *Proceedings of the Royal Society B: Biological Sciences* 2018a;**285**: 20180513.

Broeckhoven C, Mouton P Le FN, Hui C. Proximate causes of variation in dermal armour: insights from armadillo lizards. *Oikos* 2018c;**127**:1449–58.

Broeckhoven C, Du Plessis A, Hui C. Functional trade-off between strength and thermal capacity of dermal armor: insights from girdled lizards. *Journal of the Mechanical Behavior of Biomedical Materials* 2017b;**74**:189–94.

Broeckhoven C, Du Plessis A, Le Roux SG *et al.* Beauty is more than skin deep: a non-invasive protocol for *in vivo* anatomical study using micro-CT. *Methods in Ecology and Evolution* 2017c;**8**:358–69.

Brooks ME, Kristensen K, Benthem KJ *et al.* glmmTMB balances speed and flexibility among packages for zero-inflated generalized linear mixed modeling. *The R Journal* 2017;**9**:378–400.

Burnham KP, Anderson DR. Multimodel inference: understanding AIC and BIC in model selection. *Sociological Methods & Research* 2004;**33**:261–304.

Clarac F, Quilhac A. The crocodylian skull and osteoderms: a functional exaptation to ectothermy? *Zoology* 2019;**132**:31–40.

Clarac F, Goussard F, de Buffrénil V *et al.* The function(s) of bone ornamentation in the crocodylomorph osteoderms: a biomechanical model based on a finite element analysis. *Paleobiology* 2019;**45**:182–200.

Clarac F, Goussard F, Teresi L *et al.* Do the ornamented osteoderms influence the heat conduction through the skin? A finite element analysis in Crocodylomorpha. *Journal of Thermal Biology* 2017;**69**:39–53.

Clusella-Trullas S, van Wyk JH, Spotila JR. Thermal benefits of melanism in cordylid lizards: a theoretical and field test. *Ecology* 2009;**90**:2297–312.

Cox RM, Skelly SL, John-Alder HB. A comparative test of adaptive hypotheses for sexual size dimorphism in lizards. *Evolution; International Journal of Organic Evolution* 2003;**57**:1653–69.

Dacke CG, Elsey RM, Trosclair PLIII, *et al.* Alligator osteoderms as a source of labile calcium for eggshell formation. *Journal of Zoology* 2015;**297**:255–64.

Du Plessis A, Broeckhoven C, Guelpa A *et al.* Laboratory X-ray micro-computed tomography: a user guideline for biological samples. *GigaScience* 2017;**6**:1–11.

Du Plessis A, Broeckhoven C, Yadroitsev I *et al.* Analyzing nature's protective design: the glyptodont body armor. *Journal of the Mechanical Behavior of Biomedical Materials* 2018;**82**:218–23.

Ebel R, Herrel A, Scheyer TM *et al.* Review of osteoderm function and future research directions. *Journal of Zoology* 2025;**325**:1–24.

Eifler DA, Eifler MA, Eifler EN. Habitat use and movement patterns in the graceful crag lizard, *Pseudocordylus capensis*. *African Zoology* 2007;**42**:152–7.

Etterson JR, Schneider HE, Gorden NLS *et al.* Evolutionary insights from studies of geographic variation: contemporary variation and looking to the future. *American Journal of Botany* 2016;**103**:5–9.

Fick SE, Hijmans RJ. WorldClim 2: new 1-km spatial resolution climate surfaces for global land areas. *International Journal of Climatology* 2017;**37**:4302–15.

Fischer V, Bennion RF, Foffa D *et al.* Ecological signal in the size and shape of marine amniote teeth. *Proceedings. Biological Sciences* 2022;**289**:20221214.

Frýdlová P, Dudák J, Tymlová V *et al.* Hidden armour: the passive protective function of caudal osteoderms in snakes. *Journal of Morphology* 2025;**286**:e70034.

Gamelon M, Morimoto J, White HJ. Special feature: intraspecific variation in ecology & evolution. *The Journal of Animal Ecology* 2025;**94**:262–7.

Greer AE. *The Biology and Evolution of Australian Lizards*. Chipping Norton, NSW: Surrey Beatty, 2007.

Herrel A, Damme RV, Vanhooydonck B *et al.* The implications of bite performance for diet in two species of lacertid lizards. *Canadian Journal of Zoology* 2001;**79**:662–70.

Herselman YM, Mouton PlFN, van Wyk JH. The status of the races of the graceful crag lizard, *Pseudocordylus capensis* (Sauria: Cordylidae). *The Journal of the Herpetological Association of Africa* 1992;**40**:29.

Huey RB, Pianka ER. Seasonal variation in thermoregulatory behavior and body temperature of diurnal Kalahari lizards. *Ecology* 1977;**58**:1066–75.

Iacoviello F, Kirby AC, Javanmardi Y *et al.* The multiscale hierarchical structure of *Heloderma suspectum* osteoderms and their mechanical properties. *Acta Biomaterialia* 2020;**107**:194–203.

Inacio Veenstra LL, Broeckhoven C. Revisiting the thermoregulation hypothesis of osteoderms: a study of the crocodilian *Paleosuchus palpebrosus* (Crocodilia: Alligatoridae). *Biological Journal of the Linnean Society* 2022;**135**:679–91.

Janse Van Rensburg DA. Effective conservation of melanistic lizard species in the Greater Cederberg Biodiversity Corridor. Doctoral Thesis, Stellenbosch University, 2009.

Janse Van Rensburg DA, Mouton PlFN. Foraging behaviour and use of space in the graceful crag lizard, *Pseudocordylus capensis*: life on large rock surfaces. *African Journal of Herpetology* 2009;**58**:106–15.

Kéver L, Olivier D, Marghoub A *et al.* Biomechanical behaviour of lizard osteoderms and skin under external loading. *Journal of Experimental Biology* 2022;**225**:jeb244551.

Kyriazos T, Poga M. Dealing with multicollinearity in factor analysis: the problem, detections, and solutions. *Open Journal of Statistics* 2023;**13**:404–24.

Lang M. Generic relationships within Cordyliformes (Reptilia.Squamata). *Biologie* 1991;**61**:121–88.

Lawing AM, Polly PD. Geometric morphometrics: recent applications to the study of evolution and development. *Journal of Zoology* 2010;**280**:1–7.

Leitão HG, Diedericks G, Broeckhoven C *et al.* Chromosome-level genome assembly of the cape cliff lizard (*Hemicordylus capensis*). *Genome Biology and Evolution* 2023;**15**:evad001.

Losos JB, Mouton PlFN, Bickel R *et al.* The effect of body armature on escape behaviour in cordylid lizards. *Animal Behaviour* 2002;**64**:313–21.

Maisano JA, Laduc TJ, Bell CJ *et al.* The cephalic osteoderms of *Varanus komodoensis* as revealed by high-resolution X-ray computed tomography. *Anatomical Record* 2019;**302**:1675–80.

Maliuk A, Marghoub A, Williams CJA *et al.* Comparative analysis of osteoderms across the lizard body. *Anatomical Record* 2024;**307**:3191–203.

McConnachie S, Alexander GJ, Whiting MJ. Lower temperature tolerance in the temperate, ambush foraging lizard *Pseudocordylus melanotus melanotus*. *Journal of Thermal Biology* 2007;**32**:66–71.

Mitteroecker P, Schaefer K. Thirty years of geometric morphometrics: achievements, challenges, and the ongoing quest for biological meaningfulness. *American Journal of Biological Anthropology* 2022;**178**(Suppl 74):181–210.

Mouton PlFN. Aggregation behaviour of lizards in the arid western regions of South Africa. *African Journal of Herpetology* 2011;**60**:155–70.

Mouton PlFN, Van Wyk JH. Adaptive radiation in cordyliform lizards: an overview. *African Journal of Herpetology* 1997;**46**:78–88.

Mucina L, Rutherford MC. *The Vegetation of South Africa, Lesotho and Swaziland*. Pretoria: Strelitzia, 2011.

Muñoz-Nolasco FJ, Arenas-Moreno DM, Santos-Bibiano R *et al.* Evaporative water loss of some habitat-restricted Mexican lizard species. *Herpetological Conservation and Biology* 2019;**14**:54–66.

Olsson M, Shine R, Wapstra E *et al.* Sexual dimorphism in lizard body shape: the roles of sexual selection and fecundity selection. *Evolution; International Journal of Organic Evolution* 2002;**56**:1538–42.

Parusnath S. Natural History Note: Cordylidae *Smaug giganteus* (A. Smith, 1844) Sungazer: Predation. *African Herp News* 2012;**58**:13–14.

R Core Team. R: a language and environment for statistical computing. Vienna, Austria: R Foundation for Statistical Computing, 2021.

Seidel MR. The osteoderms of the American alligator and their functional significance. *Herpetologica* 1979;**35**:375–80.

Shine R. *Australian Snakes: a Natural History*. Frenches Forest: Reed New Holland, 1998.

Shine R, Branch WR, Harlow PS *et al.* Biology of burrowing asps (Atractaspididae) from Southern Africa. *Copeia* 2006;**2006**:103–15.

Shine R, Branch WR, Webb JK *et al.* Ecology of cobras from southern Africa. *Journal of Zoology* 2007;**272**:183–93.

Shuttleworth C, Mouton PlFN, van Niekerk A. Climate and the evolution of group-living behaviour in the armadillo lizard (*Ouroborus cataphractus*). *African Zoology* 2013;**48**:367–73.

Sun CY, Chen PY. Structural design and mechanical behavior of alligator (*Alligator mississippiensis*) osteoderms. *Acta Biomaterialia* 2013;**9**:9049–64.

Taft JM, Greuel J, Maritz B. Natural history note: lamprophidae *Lampophis guttatus* (A. Smith 1844) spotted house snake: diet. *African Herp News* 2017;**65**:11.

Van Wyk JH, Mouton PlFN. Reproduction and sexual dimorphism in the montane viviparous lizard, *Pseudocordylus capensis* (Sauria: Cordylidae). *South African Journal of Zoology* 1998;**33**:156–65.

Vickaryous MK, Hall BK. Development of the dermal skeleton in *Alligator mississippiensis* (Archosauria, Crocodylia) with comments on the homology of osteoderms. *Journal of Morphology* 2008;**269**:398–422.

Vickaryous MK, Sire JY. The integumentary skeleton of tetrapods: origin, evolution, and development. *Journal of Anatomy* 2009;**214**:441–64.

Williams C, Kirby A, Marghoub A *et al.* A review of the osteoderms of lizards (Reptilia: Squamata). *Biological Reviews of the Cambridge Philosophical Society* 2022;**97**:1–19.

Yang W, Chen IH, Gludovatz B *et al.* Natural flexible dermal armor. *Advanced Materials (Deerfield Beach, Fla.)* 2013;**25**:31–48.

Zamora-Camacho FJ, Reguera S, Moreno-Rueda G. Bergmann's Rule rules body size in an ectotherm: heat conservation in a lizard along a 2200-metre elevational gradient. *Journal of Evolutionary Biology* 2014;**27**:2820–8.

Zelditch M, Swiderski DL, Sheets HD, Fink WL. *Geometric Morphometrics for Biologists: a Primer*. London: Academic Press, 2004.